Colloids and Surfaces B: Biointerfaces 86 (2011) 81–86

Contents lists available at ScienceDirect

Colloids and Surfaces B: Biointerfaces

journal homepage: www.elsevier.com/locate/colsurfb

A novel dendritic surfactant for enhanced microcystin-LR detection by double amplification in a quartz crystal microbalance biosensor

Yuetong Xia, Jianping Zhang, Long Jiang*

Beijing National Laboratory for Molecular Science, Institute of Chemistry, Chinese Academy of Sciences, Beijing 100190, PR China

ARTICLE INFO

Article history:
Received 23 November 2010
Received in revised form 17 February 2011
Accepted 15 March 2011
Available online 23 March 2011

Keywords:
Microcystin-LR
Quartz crystal microbalance
Dendritic surfactant
Vesicle array
Double amplification

ABSTRACT

Enhanced sensitivity for the hepatotoxin microcystin-LR (MC-LR) was achieved in a quartz crystal microbalance (QCM) system via double amplification. For primary amplification, an innovative interface on the QCM was obtained as a matrix by the vesicle layer formed by our synthetic dendritic surfactant, bis (amidoethyl-carbamoylethyl) octadecylamine (C18N3). The vesicle matrix was then functionalised by an optimised concentration of monoclonal antibodies against MC-LR (anti-MC-LR) to detect the analyte. The results showed that a detection limit of 100 ng/mL was achieved by primary amplification. To achieve higher sensitivity, secondary amplification was implemented with anti-MC-LR gold nanoparticle (AuNPs) conjugates as probes, which lowered the detection limit for MC-LR to 1 ng/mL (the maximum concentration recommended by the World Health Organization [WHO] in drinking water for humans). The QCM immunosensor reported here has advantages such as high sensitivity, portability, simplicity, and cost-effectiveness for MC-LR detection. It would be uniquely superior compared with current MC-LR detection techniques for on-the-spot water detection. Furthermore, the methodology described here is also potentially significant in many fields for the routine monitoring of environmental and food safety.

1. Introduction

Microcystins are global cyanotoxins produced by the bloom-forming microcystis species [1]. They have been found to be harmful to humans, acting as inhibitors of protein phosphatases and as tumor promoters for acute hepatotoxicity [2]. Although not toxic to fish, microcystins can become enriched to levels that might lead to human consumption of amounts above the maximum concentration recommended for drinking water [3]. Chemically, microcystins (MCs) have over 80 variants [4] but can be essentially described as having a general cyclic structure of five amino acids. Two L-amino acids can be substituted and are used to name the particular microcystin, such as microcystin-LR (MC-LR) [5]. This variant is the most studied and toxic representative of the cyanotoxin family [1,6]. It contains leucine (L) and arginine (R) in positions 1 and 2, respectively, as shown in Fig. 1. It is the tremendous public health risk of MCs, especially MC-LR, which has focused attention on the detection of MC-LR in surface water in past decades.

A considerable number of different technologies are currently used for the measurement of MC-LR [7]. To date, high-performance liquid chromatography (HPLC) [8], mass spectrometry (MS) [9], magnetic resonance screening [10], etc., are capable of achieving detection below the 0.1-ng/mL limit, but all of these methods suffer from extremely high costs and very bulky equipment, which prevent portable measurements of MCs *in situ*. Traditional biological methods, such as enzyme-linked immunosorbent assay (ELISA) [11,12], also cannot satisfy the requirements for the routine monitoring of MC-LR, because ELISA is labor-, money- and time-consuming, despite the minimal facilities required and its high specificity and sensitivity (far below the 1-ng/mL value that the WHO stated). Thus, a sensitive, convenient and inexpensive method for MC-LR monitoring in routine is needed. To achieve this,, some work has already been implemented. For instance, Nils et al. developed an immunochromotographic lateral-flow dipstick assay for the fast and portable detection of MC-LR with a sensitivity of 5 ng/mL [13]. Wang et al. reported a simple SWNT-paper sensor for MC-LR, successfully achieving a detection limit of 0.6 ng/mL [1]. Here, we aim to combine the sensitivity and specificity of immunoassays like ELISA [3,14] with the simplicity and portability of a piezoelectric technique (quartz crystal microbalance [QCM]).

QCM is a popular transducer in immunoassays [15,16]. Immunosensors based on QCM are especially advantageous because of their low cost (minimal reagents), high portability (miniature size) and wide and routine adaptability (simple and rapid operation procedures) [17–19]. Despite these advantages, the use of QCM for the detection of trace biological targets is still encumbered by its relatively low intrinsic sensitivity [15]. Thus, extensive efforts have been made to improve its sensitivity [20–23]. For example, the sensitivity of QCM could be enhanced by surface

* Corresponding author. Tel.: +86 82612084; fax: +86 82612084.
E-mail address: jiangl@iccas.ac.cn (L. Jiang).

0927-7765/$ – see front matter © 2011 Elsevier B.V. All rights reserved.
doi:10.1016/j.colsurfb.2011.03.019

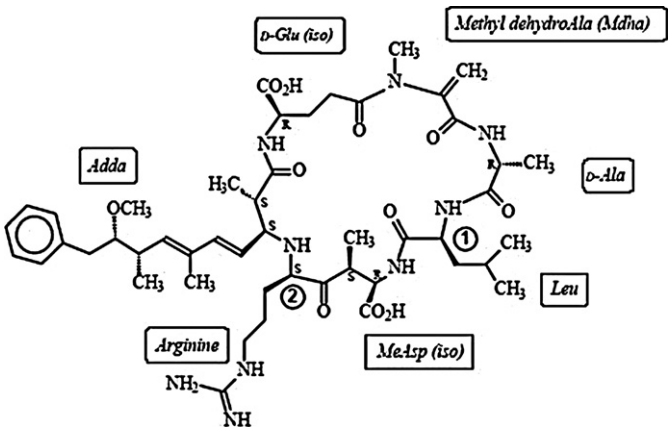

Fig. 1. Structure of MC-LR.

modification using liposome layers [24] and the mass amplification using AuNPs [18,25]. Previously, our group successfully demonstrated that QCM sensors, amplified by different sizes of AuNPs, could detect probe DNA sequences with a very sensitivity and specificity at the concentration of 10^{-16} M [26–28].

The detection of MC-LR based on QCM has been poorly researched. Our work in this paper was predicated on techniques similar to those described above but different from a report by Gorge et al. in which a comparative assay was performed with a detection limit of 1 ng/mL [29]. We utilised the vesicles formed by a novel surfactant, bis(amidoethyl-carbamoylethyl) octadecylamine (C18N3) [30], to modify the QCM surface for the primary amplification. C18N3 is extremely biocompatible with antibodies, which maintain the activity dependent on its outward-facing multi-amine head and well-structured double membrane mimicking the liposome. However, they are easier to synthesise at low cost and self-organise in water. Therefore, this vesicle coating could be better for fabricating a comparatively smart and stable piezoelectric immunosensor for toxin detection. Furthermore, AuNP-functionalised antibodies were introduced as the secondary amplification step in MC-LR detection (Scheme 1). The results showed that our QCM immunosensor had a markedly enhanced sensitivity compared with most QCM sensors and could detect MC-LR within the specified value of 1 ng/mL. Actually it should be noticed that under the liquid phase, a dissipation factor must be considered during the QCM measurement [31]. Yet, in our condition, the experiments were carried out in the gas-monitoring model following the Sauerbrey equation [21]. Also, we have already proved a good linear relationship between the frequency and the weight change in our previous work [32]. Therefore, we assume that in our paper the dissipation factor can be neglected. All the above indicated that our QCM immunosensor could be the foundation of a very simple and low-cost method for MC-LR monitoring in water. In fact, its analysis procedure with a well-functionalised chip is fast and more portable than HPLC, and it has tremendous potential for everyday environmental MC-LR monitoring. Furthermore, it is potentially significant in the field of fabricating optimum QCM-based immunosensors using surface modification.

2. Materials and methods

2.1. Apparatus and materials

2.1.1. Apparatus

8-MHz (basic frequency) AT-cut quartz crystals with electrode surfaces covered with gold (Au) and chromium (Cr) on both sides were purchased from Chenhua Co., Ltd, Shanghai, China. The thicknesses of the quartz, Cr and Au were 0.5 mm, while their total diameter was 12 mm. The quartz crystal microbalance was driven with a 9-V direct current (VDC). The resonant frequency was monitored with a frequency counter. Scheme 1 shows a practical schematic of the entire QCM detection system.

2.1.2. Materials

Monoclonal antibodies (mAb) against MC-LR (anti-MC-LR), MC-LR, and microcystin-RR (MC-RR) were all purchased from the Express Technology Co., Ltd., Beijing, P.R.C. Anti-human-IgG and human IgG were purchased from Ke Baiao Biocompany, Beijing. Glutaraldehyde (GA), N-(3-dimethylaminopropyl)-N′-ethylcarbodiimide hydrochloride (EDC), N-hydroxysuccinimide (NHS), 16-mercaptohexadecanoic acid and bovine serum albumin (BSA) were purchased from Sigma–Aldrich. C18N3 was synthesised according to the procedure of Wang et al. [30]. All other chemicals, such as sodium citrate and $HAuCl_4{\cdot}3H_2O$, were analytical regent-grade and obtained from the Beijing Chemical Reagent Company. The colloidal gold with a diameter of 12 nm was prepared following the procedure reported by Mirkin et al. [33]. Phosphate buffered saline (PBS) was prepared: 137 mM NaCl, 2.7 mM KCl, 10 mM Na_2HPO_4, 1.47 mM KH_2PO_4, pH 7.4. The ultrapure water (18.2 MΩ) was produced using a Millipore-Q water system.

2.2. Comparison of the active QCM surfaces

The crystal was cleaned by pipetting 20 μL of fresh piranha solution (one part 30% H_2O_2, three parts H_2SO_4) on the gold electrode surface for 3 min followed by rinsing with Millipore-Q water and drying with N_2. The crystal's frequency was monitored and recorded in air at room temperature. To compare the responses of the analytes, aside from the antibody immobilisation on the C18N3-vesicle-modified QCM, two additional methods of antibody immobilisation were investigated: immobilising antibodies on a self-assembled monolayer (SAM) of thiourea and on the bare QCM surface. Here, we detected human IgG (h-IgG) instead of MC-LR by anti-h-IgG, because we assumed that this was more

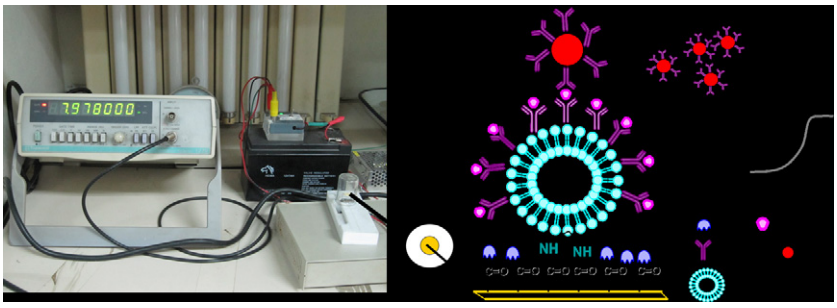

Scheme 1. Apparatus and schematic depiction of MC-LR detection by the QCM immunosensor.

environmentally friendly and cost-effective but had the same detection efficacy.

The C18N3-modified surface was prepared as follows. Briefly, 10 μL of ethanol solution containing 16-mercaptohexadecanoic acid was dropped onto the clean crystal surface. After incubation for 30 min at room temperature and cleaning and drying by N_2, the modified wafer was activated by the mixing solutions of 100-mM EDC and 100-mM NHS for 1 h. Subsequently, the solution of C18N3 vesicles was added to form the "liposome array" [17,34]. The C18N3 vesicles were prepared according to the protocol of Wang [30] with the following minor change: C18N3 was dissolved in PBS buffer with pH 6.8 to attain a concentration of 5 mM. (The molecular structure and its morphology in solution are shown in Fig. S3 in the supplemental material.) The vesicle solution was then sonicated for 10 min in boiling water and placed into a refrigeration for 10 min at 4 °C. The activated surface was then immersed in 30 μL of C18N3 vesicle solution at a concentration of 5 mM for 1 h before GA was used to activate its amine groups for another hour at 37 °C.

The SAM of thiourea was immobilised on the gold surface of QCM according to the protocol of Loyprasert et al. [35]. Briefly, 50 μL of PBS solution with thiourea at a concentration of 250 mM was pipetted onto the gold slide and was adsorbed for 48 h in the dark. The surface was then incubated with the solution of GA for 1 h after washing the crystal with ethanol and pure water at 37 °C.

The three types of QCM surfaces were then all incubated in 20 μL of PBS solution with anti-h-IgG (10 μg/mL) for 2 h at 37 °C and then blocked with 1% BSA in PBS solution to avoid nonspecific absorption. After washing with PBS and pure water, the crystal was dried with N_2, and its frequency change was recorded in air at the room temperature. Finally, 10 μL of human IgG solution at a concentration of 10 μg/mL were pipetted onto the bioactive surfaces and allowed to react at 37 °C for 2 h.

2.3. Preparation of the anti-MC-LR immobilised QCM surface

The same protocol was carried out as described above for the $C_{18}N_3$-modified QCM surface. Only the activated surface was allowed to conjugate with a 10 μL of solution containing the anti-MC-LR. To optimise the analytical parameters, different concentrations (5, 10, 20, 40, 50, 70, 90, and 100 μg/mL) of anti-MC-LR were investigated to detect the same amount of MC-LR (1 μg/mL). In our experiments, we chose PBS with a pH of 7.4 as the buffer solution and 37 °C as reaction temperature, as selected by Wang et al. [1] for MC-LR. The optimal antibody-functionalised QCM surface then would react with MC-LR in the subsequent steps.

2.4. Preparation of the anti-MC-LR-colloidal gold conjugate

The anti-MC-LR-colloidal gold conjugate (i.e. the antibody-functionalised Au nanoparticles) was prepared as described in literature [25], with minor changes as follows: While gently stirring, the anti-MC-LR solution (containing 20 μg of antibody) was added to 1 mL of colloidal gold solution (adjusted to pH 9.0 with K_2CO_3). The mixture was incubated at room temperature for 0.5 h. Then, 200 μL of 5% BSA was added to the mixture to stabilise the colloidal gold solution, and the mixture was incubated for an additional 0.5 h. After centrifugation at 10,000 rpm for 45 min, two phases were obtained: the clear, pink supernatant of unbound antibody and the dark red, loosely packed sediment of conjugates. The supernatant was discarded, and the soft sediment of the conjugate was rinsed by resuspension in 1 mL of BSA in PBS buffer and collected after a second centrifugation at 10,000 rpm for 45 min. Finally, the conjugate was resuspended in 1 mL of PBS with 0.1% BSA to minimise nonspecific absorption and increase the stability of the conjugate during the immunoassay. The conjugates were able to be stored at 4 °C for more than 1 month without any significant decrease in activity. An ultraviolet–visible (UV–vis) spectrometer, Fourier transmittance infrared (FT-IR) spectra, transmission electronic microscopy (TEM) and dynamic light scattering (DLS) were used to characterise the immunocomplex. (The details of these apparatuses are listed in Supplemental material.)

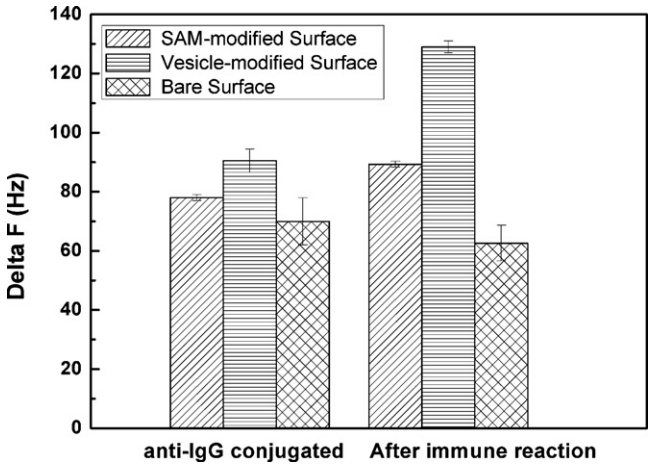

Fig. 2. Comparison of the three methods of antibody immobilization and their performances in recognizing events.

2.5. Analytical procedures

Solutions of MC-LR (10 μL) at different concentrations (1 ng/mL, 10 ng/mL, 50 ng/mL, 100 ng/mL, and 1 μg/mL) were applied to the anti-MC-LR-functionalised vesicle layer on the QCM surface. After the immune reaction at 37 °C for 1.5 h, the anti-MC-LR-colloidal gold conjugates were diluted two times [25] and were added and allowed to react for another 1.5 h at 37 °C. As controls, BSA and MC-RR were also investigated at the same experimental conditions. After each adsorption, the crystal was always washed and dried with N_2, and its frequency change was monitored and recorded in air.

3. Results and discussion

3.1. Optimisation of the antibody immobilisation method on the QCM surface

To determine whether the performance of our C18N3 vesicle layer was improved compared to the bare and SAM-modified surfaces, parallel experiments were carried out to detect h-IgG. Fig. 2 shows the comparison of the responses (1) after antibody immobilisation by three different immobilisation methods and (2) after exposure of the anti-h-IgG-functionalised QCM to a solution 10-μg/mL h-IgG in PBS. Of the three methods, it was found that the anti-h-IgG linked to the C18N3-modified surface yielded a maximum frequency change of 90 ± 3 Hz after antibody immobilisation and then 129 ± 2 Hz after IgG recognition. This result could probably be explained as follows: a highly efficient protein assay requires high coverage of biofunctional molecules, which is why the SAM method [17] has recently become the focus of research on modifying various surfaces used in biological applications. However, in contrast to a monolayer array, a liposome-mimicking array (i.e., a C18N3 vesicle array) would be superior in terms of signal amplification due to its high surface area and 3D interactions between the layer and the target molecules [34]. Additionally, the biocompatible membranes of the C18N3 vesicles would help maintain protein bioactivity with good stability and reproducibility. Therefore, a stronger response was attained in the recognising process,

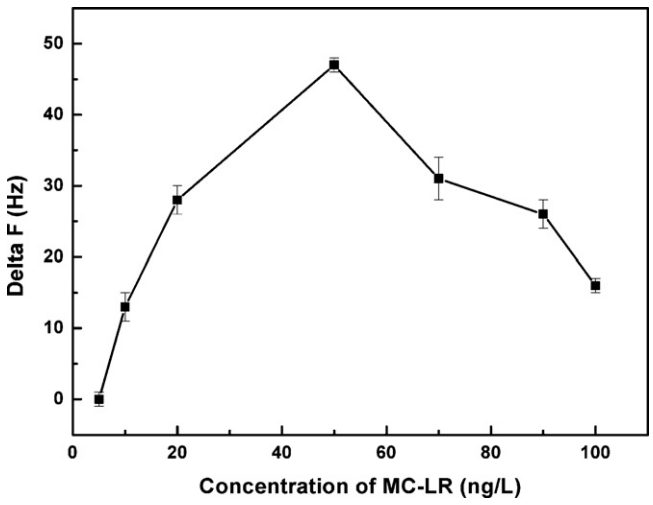

Fig. 3. Optimization of the anti-MC-LR concentration for MC-LR detection.

which would thus result in a higher sensitivity. For the bare QCM surface, both the immobilisation of the antibody and the recognition signals were found to be at a minimum, because less directional immobilisation without any stabiliser might lead to a loss of activity and exposed active sites. Briefly, all of the results suggest that the C18N3-vesicle-array-modified QCM surface should be a suitable method to immobilise antibodies. Furthermore, compared to phospholipid assemblies, our synthesised vesicles are more cost-effective and easier to prepare in water.

3.2. Optimisation of anti-MC-LR on the C18N3-modified surface

The sensitivity and selectivity of piezoelectric detection can be very strongly influenced by the immobilised antibodies on the surface. Although there should be as many antibodies as possible exposed for antigen recognition, too many antibodies will decrease the number of binding events through a hindrance effect and thus lower the detection limit [23]. Therefore, the optimum concentration of anti-MC-LR was determined for the detection of 1 μg/mL MC-LR. Various concentrations of anti-MC-LR were investigated under the same experimental conditions. The results in Fig. 3 showed that, for the anti-MC-LR concentrations up to 50 μg/mL, more antibodies were loaded on the surface, which led to a larger signal produced by the QCM. This could be simply attributed to more antibodies exposing more active sites for MC-LR recognition. However, when the amount of the anti-MC-LR loaded on the surface was increased further, as demonstrated by the increased frequency shifts (see Supplemental Fig. S1), the binding interaction between the anti-MC-LR and MC-LR seemed to be impaired. This result could be explained by larger numbers of antibodies immobilised on the QCM surface decreasing the space for the MC-LR to approach and affect the immune interactions, even though the MC-LR molecule is small. This model strongly agrees with the previous literature [17,19]. Therefore, the optimum concentration of the anti-MC-LR supported by our C18N3-modified QCM was found to be 50 μg/mL. The C18N3 vesicle-modified QCM sensing interface with 50 μg/mL of anti-MC-LR thus served as the primary amplification for the detection of MC-LR in the subsequent experiments.

3.3. Characterisation of the anti-MC-LR colloidal-gold nanoparticle

The modification of anti-MC-LR on AuNPs was confirmed by UV–vis spectrometry and FT-IR spectroscopy. As shown in Fig. S4, the absorption peak of the gold-anti-MC-LR nanoparticles was just appreciably broadened and slightly red-shifted compared with bare AuNPs, suggesting that most of the AuNPs were well dispersed even when conjugated with the anti-MC-LR. This conclusion was supported by the TEM image of the anti-MC-LR colloidal-gold nanoparticles shown in the inset of Fig. S4. The FT-IR spectrum was also utilised to characterise the organic functional groups. Fig. S5 shows that the gold-anti-MC-LR nanoparticles had the obvious absorption peaks of the anti-MC-LR (for example, one at 1658 cm^{-1} and one at 1530 cm^{-1}, which were attributed to the vibrations of amide and amide, respectively). These peaks are also features of the absorptions of the typical functional groups of the antibodies. Therefore, we concluded not only that the anti-MC-LR successfully coated the AuNP surfaces but also that the basic features of the anti-MC-LR were maintained after conjugation to the AuNPs. The subsequent experiments could then determine whether the anti-MC-LR-colloidal gold nanoparticles could effectively detect MC-LR.

Furthermore, to gain an insight into the properties of the AuNP surface linked to the anti-MC-LR, electrophoresis experiments using DLS were carried out to determine the superficial electricity by measuring the zeta potential. The zeta potential of the AuNPs at the beginning was -37 ± 3 mV (Supplemental Table S1). After modification with the anti-MC-LR, the value changed to -16.5 ± 1 mV, which was consistent with the original value of -16.7 ± 1.5 mV determined for the anti-MC-LR. Therefore, we concluded that the surfaces of the AuNPs were fully covered by the anti-MC-LR.

3.4. Response of the QCM immunosensor to MC-LR

The immunoassay experiments in this study were carried out in a gas-monitoring model. Fig. 4 shows the typical frequency changes of the functionalised quartz crystal, which result from a cascade of interactions with the anti-MC-LR, MC-LR, and gold-anti-MC-LR conjugates. As shown in Fig. 4 (curve a), a frequency change of about 96 ± 3 Hz was observed after the C18N3-modified surface was conjugated with 50 μg/mL of anti-MC-LR to saturation within 2.5 h. After the nonspecific sites were blocked with a 1% BSA solution, the association of 500 ng/mL MC-LR was completed within 1.5 h and led to an additional frequency change of about 37 ± 5 Hz as primary amplification. In contrast, the addition of 500 ng/mL BSA led to a frequency shift of only 8 ± 2 Hz (Fig. 4, curve b). These results indicated that all of the active sites created by the C18N3 vesicles were saturated with the anti-MC-LR with almost no nonspecific absorption. The treatment with the secondary amplification probes (the gold-anti-MC-LR conjugates) yielded a frequency change of about 125 ± 5 Hz within 2.5 h (Fig. 4, curve c), indicating that the binding created significant amplification for the rapid sensing of MC-LR. Furthermore, Fig. 4 (curve c) shows that the direct treatment of the sensing interface with the secondary amplification probe only gave a frequency change of 28 ± 4 Hz, which can be attributed to the nonspecific association of the protein with the interface. After applying MC-RR (a variant of MC-LR; see Supplemental Fig. S2 for the structure) to our immunosensor with double amplification, a small change of 45 ± 3 Hz was obtained, as expected (Fig. 4, curve d). These results revealed that our amplification procedure for immunosensing were both highly specific and sensitive.

3.5. Performance of the novel immunosensor with double amplification

The frequency shifts resulting from the sensing of the MC-LR analyte at different concentrations are shown in Fig. 5. The primary amplification by the C18N3-modified QCM surface and the secondary amplification using the gold-anti-MC-LR conjugate collectively enabled the sensing of MC-LR in a concentration range of 1 ng/mL to 1 μg/mL. A satisfactory frequency response was obtained and is shown in Fig. 2 (curve c). In the absence of

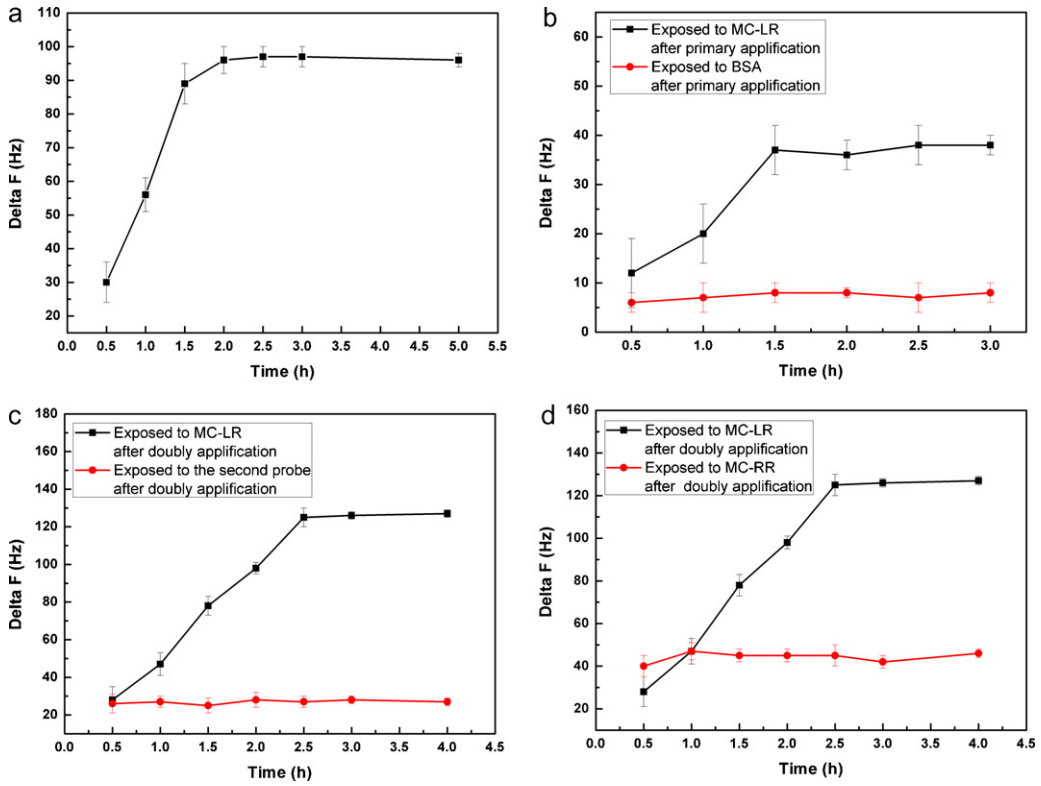

Fig. 4. Dynamic QCM responses of a cascade of interactions. (a) after the anti-MC-LR antibody linked to the C18N3-modified surface. (b) after the primary amplification and further exposure to 500 ng/mL MC-LR or BSA. (c) after a double amplification and further exposure to 500 ng/mL MC-LR or the pure secondary probes. (d) Comparison of the exposure to 500 ng/mL MC-LR or MC-RR after a double amplification.

amplification (the anti-MC-LR immobilised on the SAM-modified QCM surface), a frequency response of only 15 ± 3 Hz was detected at an MC-LR concentration as high as 100 ng/mL (Fig. 5, curve a). However, a solution of MC-LR at the same concentration was successfully detected using the two amplification procedures to obtain a frequency response of 28 ± 5 Hz for the primary amplification step and 98 ± 2 Hz after double amplification (Fig. 5, curves b and c). For MC-LR concentrations below 100 ng/mL (1 ng/mL, 10 ng/mL, and 50 ng/mL), almost no obvious responses were observed on the QCM surface only treated by primary amplification (Fig. 5, curve b). However, frequency shifts of 45 Hz, 56 Hz, and 78 Hz were successfully obtained for MC-LR concentrations of 1 ng/mL, 10 ng/mL, and 50 ng/mL, respectively, using the QCM immunosensor after the secondary amplification (Fig. 5, curve c). Additionally, the correlation curve in Fig. S6 sets the quantitative base for the determination of an unknown MC-LR concentration. All of these results indicate that the sensitivity and the detection limit of the novel doubly amplified immunosensor were dramatically improved compared with the direct QCM-based immunosensor.

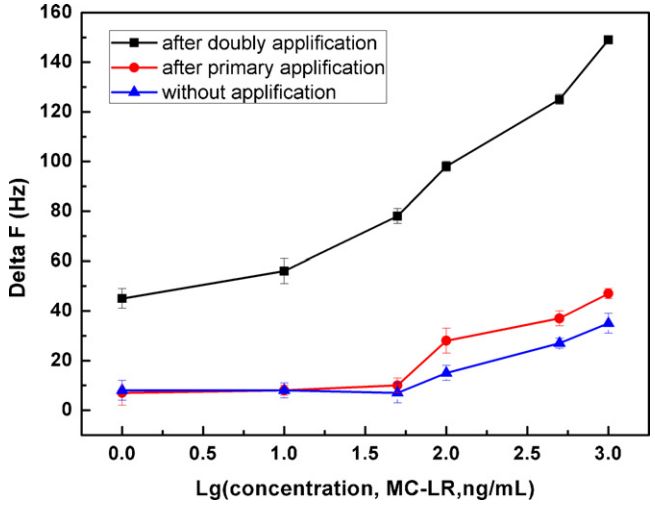

Fig. 5. Performance of the QCM immunosensor after a double amplification approach for MC-LR detection.

4. Conclusions

An immunocomplex of a gold-anti-MC-LR conjugate and a vesicle layer formed by the new surfactant C18N3 were successfully combined to produce a novel QCM-based MC-LR immunosensor. High coverage and effective immobilisation of the antibody were achieved using a lipid-mimicking vesicle double layer coated on the QCM surface as primary amplification. This modification lowered the limit of MC-LR detection of the QCM to 100 ng/mL. Furthermore, utilising a synthesised surfactant instead of commercial phospholipids to modify the QCM interface would greatly reduce the expense for the sensor manufacture. Variable substitutions of lipids with different morphologies and traits would affect the detection efficiency of the QCM immunosensor and merits more attention when developing the high-sensitivity QCM biosensors in the future. Furthermore, when coupled with the C18N3 vesicles, the use of gold-anti-MC-LR conjugates as the secondary amplification probe was shown to provide a significant enhancement in the sensing sensitivity and was able to lower the detection limit of MC-LR to 1 ng/mL. This type of assay can be easily implemented and at a low cost, indicating that this method, when combined with simple QCM, is suitable for field applications in the monitoring and detection of water pollution. Based on our previous work showing that the amplification effect is influenced by the size of AuNPs,

studies investigating the optimum nanoparticle size for MC-LR on QCM are still ongoing, and more sensitive detection is expected in the future. This novel method of producing a QCM immunosensor could potentially contribute greatly to today's urgent demands for the routine monitoring of water and food safety.

Acknowledgements

This research is supported by the Chinese Academy of Sciences (KJCX2-YW-H18) and the National Sci-Tech Major Special Item for Water Pollution Control and Management (2009ZX075287-007-03).

Appendix A. Supplementary data

Supplementary data associated with this article can be found, in the online version, at doi:10.1016/j.colsurfb.2011.03.019.

References

[1] L. Wang, W. Chen, D. Xu, B.S. Shim, Y. Zhu, F. Sun, L. Liu, C. Peng, Z. Jin, C. Xu, N.A. Kotov, Nano Lett. 9 (2009) 4147.
[2] T. Lambert, C. Holmes, S. Hrudey, Environ. Rev. 2 (1994) 167.
[3] P. Lindner, R. Molz, E.Y. George, H. Wolf, Anal. Chim. Acta 636 (2009) 218.
[4] J. Sheng, M. He, H. Shi, Anal. Chim. Acta 603 (2007) 111.
[5] M. Gao, C. Deng, Z. Fan, N. Yao, X. Xu, P. Yang, X. Zhang, Small 3 (2007) 1714.
[6] H.W. Yu, J. Lee, S. Kim, G. Nguyen, I. Kim, Anal. Bioanal. Chem. 394 (2009) 2173.
[7] A. Tillmanns, F. Pick, R. Aranda-Rodriguez, Environ. Toxicol. 22 (2007) 132.
[8] L. Lawton, C. Edwards, G. Codd, Analyst 119 (1994) 1525.
[9] T. Sano, K. Nohara, F. Shiraishi, K. Kaya, Int. J. Environ. Anal. Chem. 49 (1992) 163.
[10] W. Ma, W. Chen, R. Qiao, C. Liu, C. Yang, Z. Li, D. Xu, C. Peng, Z. Jin, C. Xu, S. Zhu, L. Wang, Biosens. Bioelectron. 25 (2009) 240.
[11] F. Chu, X. Huang, R. Wei, J. Assoc. Off. Anal. Chem. 73 (1990) 451.
[12] J. Sheng, M. He, H. Shi, Y. Qian, Anal. Chim. Acta 572 (2006) 309.
[13] N. Tippkötter, H. Stückmann, S. Kroll, G. Winkelmann, U. Noack, T. Scheper, R. Ulber, Anal. Bioanal. Chem. 394 (2009) 863.
[14] J. Zhang, J. Lei, C. Xu, L. Ding, H. Ju, Anal. Chem. 82 (2009) 1117.
[15] S. Kurosawa, M. Nakamura, J.W. Park, H. Aizawa, K. Yamada, M. Hirata, Biosens. Bioelectron. 20 (2004) 1134.
[16] S. Kurosawa, J.W. Park, H. Aizawa, S.I. Wakida, H. Tao, K. Ishihara, Biosens. Bioelectron. 22 (2006) 473.
[17] R. Hao, D.X. Wang, e. Zhang, G. Zuo, H. Wei, R. Yang, Z. Zhang, Z. Cheng, Y. Guo, Z. Cui, Y. Zhou, Biosens. Bioelectron. 24 (2009) 1330.
[18] D.Q. Tang, D.J. Zhang, D.Y. Tang, H. Ai, J. Immunol. Methods 316 (2006) 144.
[19] S. Carrara, L. Benini, V. Bhalla, C. Stagni, A. Ferretti, A. Cavallini, B. Ricc, B. Samor, Biosens. Bioelectron. 24 (2009) 3425.
[20] E. Baldrich, O. Laczka, F.J. Del Campo, F.X. Muñoz, J. Immunol. Methods 336 (2008) 203.
[21] W. Lu, L. Lin, L. Jiang, Biosens. Bioelectron. 22 (2007) 1101.
[22] H. Wang, C. Wang, C. Lei, Z. Wu, G. Shen, R. Yu, Anal. Bioanal. Chem. 377 (2003) 632.
[23] J.W. Park, S. Kurosawa, H.S. Aizawa, i. Wakida, S. Yamada, K. Ishihara, Sens. Actuators B 91 (2003) 158.
[24] H.Y. Lee, H.S. Jung, K. Fujikawa, J.W. Park, J.M. Kim, T. Yukimasa, H. Sugihara, T. Kawai, Biosens. Bioelectron. 21 (2005) 833.
[25] X. Chu, Z.-L. Zhao, G.-L. Shen, R.Q. Yu, Sens. Actuators B 114 (2006) 696.
[26] T.J. Liu, a. Tang, L. Jiang, Biochem. Biophys. Res. Commun. 313 (2004) 3.
[27] T.J. Liu, A. Tang, M. Han, L. Jiang, Biochem. Biophys. Res. Commun. 304 (2003) 98.
[28] T.J. Liu, A. Tang, L. Jiang, Biochem. Biophys. Res. Commun. 295 (2002) 14.
[29] R.D. Vaughan, E. Geary, M. Pravda, G.G. Guilbault, Intern. J. Environ. Anal. Chem. 83 (2003) 555.
[30] W. Wang, W. Lu, L. Jiang, J. Phys. Chem. B 112 (2008) 1409.
[31] M.V. Voinova, M. Jonson, B. Kasemo, Biosens. Bioelectron. 17 (2002) 835–841.
[32] S. Li, X. Li, J. Zhang, Y. Zhang, J. Han, L. Jiang, Colloid Surface A 364 (2010) 158.
[33] C. Mirkin, R. Letsinger, R. Mucic, J. Storhoff, Nature 382 (1996) 607.
[34] Y.K. Jung, T.W. Kim, C. Jung, D.Y. Cho, H.G. Park, Small 4 (2008) 1778.
[35] S. Loyprasert, P. Thavarungkul, P. Asawatreratanakul, B. Wongkittisuksa, C. Limsakul, P. Kanatharana, Biosens. Bioelectron. 24 (2008) 78.